Investigation of Solid-State Reactions Using Variable Temperature X-Ray Powder Diffractometry. I. Aspartame Hemihydrate

Suneel Rastogi,[1,2] Marek Zakrzewski,[3,4] and Raj Suryanarayanan[1,5]

Received August 29, 2000; accepted December 12, 2000

Purpose. The object of this study was to demonstrate the applicability of variable temperature X-ray powder diffractometry (XRD) to investigate solid-state reactions using aspartame as a model compound.
Methods. Aspartame exists as a hemihydrate (ASH) under ambient conditions and converts to aspartame anhydrate (ASA) at ~130°C. ASA on further heating to ~180°C undergoes decomposition (intramolecular cyclization) to form a diketopiperazine derivative (DKP). The dehydration as well as the decomposition kinetics were studied isothermally at several temperatures. The unique feature of this technique is that it permits simultaneous quantification of the reactant as well as the product.
Results. While the dehydration of ASH appeared to follow first-order kinetics, the cyclization of ASA was a nucleation controlled process. The rate constants were obtained at various temperatures, which permitted the calculation of the activation energies of dehydration and cyclization from the Arrhenius plots. The activation energy of dehydration was also calculated according to the method described by Ng (*Aust. J. Chem.,* **28**:1169–1178, 1975) and the two values were in good agreement.
Conclusions. The study demonstrates that XRD is an excellent complement to thermal analysis and provides direct information about the solid-states of various reaction phases.

KEY WORDS: kinetics; solid-state reaction; X-ray powder diffractometry; aspartame; dehydration; decomposition.

INTRODUCTION

The present investigation is concerned with two types of solid-state decomposition reactions. The first type involves loss of solvent of crystallization while the second is a chemical decomposition reaction. The kinetics of solid-state decomposition reactions is conventionally studied by thermoanalytical techniques (1,2) such as thermogravimetric analysis (TGA) and differential scanning calorimetry (DSC). However, these techniques have several drawbacks. They do not unambiguously identify crystalline solid phases and provide little or no information about their degree of crystallinity (3). Since intermediate phases (if any) may not be readily identified, these techniques are not necessarily useful for discerning the reaction mechanism. When two or more gaseous products are simultaneously evolved, thermal analysis alone is not very helpful in the study of reaction kinetics (4). In such cases, thermal analysis should be used in conjunction with other techniques for evolved gas analysis (e.g., infrared spectroscopy, mass spectroscopy or gas chromatography). It is often realized that solid-state reactions take place through complex mechanisms involving intermediates and the same end product is obtained through multiple pathways (5,6). In such cases, thermoanalytical techniques yield complex profiles due to overlapping thermal events. Often, it is difficult to separate the reaction steps and study the kinetics of the individual steps.

Variable temperature X-ray powder diffractometry is a technique where X-ray diffraction patterns are obtained while the sample is subjected to a controlled temperature program. While the weight and the heat flow in the sample can be monitored using TGA and DSC respectively, XRD provides information about alterations in the solid-state of the sample. Thus, XRD is an excellent complement to thermoanalytical techniques. Numerous transitions such as dehydration, polymorphic transformation, formation of amorphous phase and recrystallization can be observed using variable temperature XRD. Since the solid-state of the intermediates (if any) can be readily characterized, the technique has the potential to provide information about the reaction mechanism. For example, the dehydration of theophylline monohydrate was investigated by this technique (7). The study revealed the formation of a metastable anhydrous phase, which then transformed to the stable anhydrate. Recent advances in instrumentation have enabled simultaneous and independent control of the temperature and the water vapor pressure in the sample chamber (4,8).

The object of this investigation was to develop and validate an XRD method to study the kinetics of a multi-step decomposition of a pharmaceutical solid. Two reactions were studied: the dehydration of aspartame hemihydrate to form anhydrous aspartame followed by its cyclization to form DKP. Aspartame hemihydrate was used as the model compound since its dehydration followed by decomposition has been studied in detail (9–12). Leung and Grant demonstrated that in the solid-state, anhydrous aspartame (ASA) undergoes intramolecular cyclization to form a single crystalline product (9). This involves nucleophilic attack of the N-terminal nitrogen on the carbonyl group of the phenylalanyl residue yielding a diketopiperazine derivative (DKP: 3-carboxymethyl-6-benzyl-2,5-diketopiperazine, $C_{13}H_{14}O_4N_2$) along with the evolution of gaseous methanol. State-of-the-art instrumentation was used, the features of which are described below. (i) A high temperature attachment that permitted us to carry out the reactions at temperatures ranging from room temperature to 300°C. (ii) A position sensitive detector (PSD), which enabled very rapid data collection. This was invaluable while monitoring fast reactions. For example, even in a fast reaction that was complete in 15 minutes, over 10 data points were obtained. (iii) Reliable data (peak) analysis program, which was particularly useful to decompose asymmetric and overlapping X-ray peaks.

MATERIALS AND METHODS

Aspartame hemihydrate ($C_{14}H_{18}O_5N_2 \cdot 0.5H_2O$) was a generous gift from the NutraSweet Kelco Co., Mount Prospect, IL.

[1] College of Pharmacy, 308, Harvard St. S.E., University of Minnesota, Minneapolis, Minnesota 55455.
[2] Present address, Forest Laboratories, Inc., 300, Prospect St., Inwood, New York 11096.
[3] Philips Analytical X-ray, Almelo, The Netherlands.
[4] Present address, Advanced Solid State Characterization, Inc., 520 Anthony's Drive, Exton, Pennsylvania 19341.
[5] To whom correspondence should be addressed. (e-mail: surya001@tc.umn.edu)

0724-8741/01/0300-0267$19.50/0

Karl Fischer Titrimetry

The water content of the samples was determined using a Karl Fischer titrimeter (Model CA-05 Mitsubishi Moisture Meter).

Hot Stage Microscopy

The sample was dispersed on a slide, a drop of high boiling silicon oil (Aldrich Chemical Co.) was added and then a cover slip was placed over it. It was heated at 10°C/min on a hot stage (Mettler FP 80, Mettler Instrument corporation) mounted on an optical microscope (Wild M3Z, Wild Heerbrugg) and observed continuously.

Variable Temperature XRD

A wide angle X-ray diffractometer (Model XDS 2000, Scintag) with a variable temperature attachment was used. This included a heat and temperature controller (Micristar, Model 828D, R. G. Hansen and Associates) which had a working temperature range of -190 to 300°C. ASH was filled in a copper holder and exposed to Cu Kα radiation (45 kV ×40 mA) in a continuous temperature step scan operation mode at a heating rate of $10°C \cdot min^{-1}$. During the XRD run, the sample was maintained under isothermal conditions. The samples were scanned over the angular range of 5 to 40° 2Θ at $5° \ 2\Theta \cdot min^{-1}$ and XRD patterns were obtained at the desired temperatures. The step size was 0.03°2Θ.

Reaction Under Isothermal Conditions

The studies were carried out in a θ-θ X-ray powder diffractometer (Philips X'Pert-MPD system) with a non-ambient attachment (model TTK-2 HC, Anton Paar) and a position sensitive detector (RAYTECH) in the static mode. Since the sample stage is held in a fixed position in a Θ-Θ diffractometer, it is ideally suited to monitor solid-state reactions. The sample stage was aligned using an alignment tool made up of a flat sheet of a single crystal of silicon. The hot stage was calibrated with stearic acid. Stearic acid was observed to melt over the temperature range of 67–69°C which was in excellent agreement with its reported melting temperatures.

The TGA curve of ASH revealed two steps of weight loss which were attributed to (9): (i) the dehydration of ASH to aspartame anhydrate (ASA) at ~130°C and (ii) intramolecular cyclization of ASA to form a diketopiperazine derivative (DKP) at ~180°C. Our first interest was to monitor the dehydration of ASH under isothermal conditions. ASH powder was filled into an X-ray holder, maintained isothermally at the desired temperature and exposed to Cu Kα radiation at regular intervals. Variable temperature XRD of ASH (Fig. 1) revealed that the peaks unique to ASH (at 15.9 and 16.4°2Θ) and ASA (17.1°2Θ) did not significantly overlap in the range of 15.2 to 17.8°2Θ. This range was therefore selected for monitoring the kinetics of dehydration of ASH. Thus, the XRD patterns were obtained as a function of time over this angular range. The quantification of ASH was based on the sum of the integrated intensities of the peaks at 15.9 and 16.4°2Θ, while the intensity of the 17.1°2Θ peak was used to quantify ASA. Since the concentrations of the crystalline reactant as well as the product were simultaneously monitored,

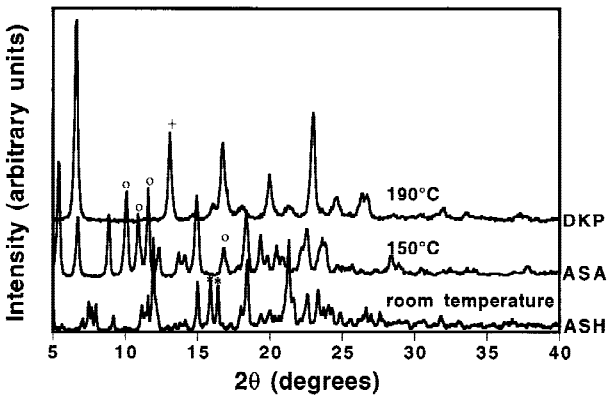

Fig. 1. Variable temperature XRD of aspartame hemihydrate. While the XRD patterns were obtained at several temperature, only the patterns at selected temperatures are provided. '*', 'o' and '+' denote the peaks unique to aspartame hemihydrate (ASH), aspartame anhydrate (ASA) and diketopiperazine derivative (DKP) respectively.

mass balance calculations of the crystalline phases were possible at each time point. The data collection time in the position sensitive detector ranged between 30 and 120 seconds; slower reactions permitted data collection over longer time periods. The experiments were repeated at several temperatures in the range of 106 to 124°C. At the end, in order to confirm that the reaction had gone to completion, the temperature was increased to 150°C, held for 2 minutes, and the XRD pattern was obtained. At this temperature, based on the TGA results, rapid and complete dehydration of ASH is expected.

The dehydration of ASH at 150°C resulted in highly crystalline ASA. Our next interest was to investigate the solid-state decomposition of ASA to form DKP. The sample temperature was increased and maintained at the desired value. XRD patterns were obtained over the angular range of 8.5 to 14°2θ at regular time intervals. The peaks unique to ASA (sum of the integrated intensities of the peaks at 10.2, 11.0 and 11.8°2Θ) and DKP (13.0°2Θ) were used for their quantification. As in the dehydration step, the detector exposure time ranged between 30 and 120 seconds depending on the reaction rate. The reaction was studied at several temperatures in the range of 160 to 185°C. As before, mass balance calculations of the crystalline phases were possible at each time point.

There were several complicating factors in the quantitative analyses. In ASH - ASA as well as ASA - DKP mixtures, there was some overlapping of peaks, during the intermediate stages of the reaction. The peaks were decomposed using software provided by Philips (Philips Profit). The second problem was due to asymmetric peak profiles. Using pure phases of ASH, ASA and DKP, profile fitting of the individual peaks of interest was accomplished using split Pearson VII function. The function profile parameters so obtained were used during peak decomposition in mixtures. These parameters were not allowed to be refined during their analyses. Thus, the software enabled the determination of the areas of asymmetric and overlapping peaks. Appropriate background subtraction was also performed (13). Detailed studies were also carried out to ensure that there were no major errors in phase quantification due to preferred orientation (14).

RESULTS AND DISCUSSION

The XRD pattern of aspartame hemihydrate (ASH) was very similar to that of a hemihydrate, reported in the literature as form II (11,12). The water content, determined by KFT, was 3.7% w/w, which was higher than the stoichiometric water content of 3.0% w/w for the hemihydrate ($C_{14}H_{18}O_5N_2$ $0.5H_2O$). Thus, the sample was a hemihydrate with some sorbed water. The DSC and TGA curves reveal that ASH dehydrated at ~130°C to form anhydrous aspartame (ASA) which on further heating, undergoes intramolecular cyclization to form a diketopiperazine derivative (DKP) at ~180°C (9).

$$\text{ASH} \xrightarrow[-H_2O]{(130^\circ C)} \text{ASA} \xrightarrow[-CH_3OH]{(180^\circ C)} \text{DKP}$$

When ASH was subjected to variable temperature XRD, it became evident that the powder patterns of ASH, ASA and DKP were different from one another (Fig. 1). Thus, the dehydration and the cyclization steps resulted in a change in lattice structure.

Investigation of Reaction Kinetics

The kinetics of many solid-state reactions can be described by the general relation, $f(\alpha) = kt$, where α is the mole fraction of solid that has reacted at time t and k is the rate constant. Usually, the study of kinetics of decomposition begins by plotting α versus t. The data from these plots is then fitted to several kinetic equations, which are based on different assumptions for the reaction mechanisms and the geometry of the reacting particles. The kinetics of solid-state reactions can be classified into (i) diffusion controlled, (ii) phase boundary controlled and (iii) nucleation and growth controlled reactions (15). The values of $f(\alpha)$ are plotted against t for the kinetic equations and the best fitting straight line is used to calculate the value of rate constant. It should be realized that simply fitting the data to a kinetic model does not confirm a particular reaction mechanism. However, based on the most likely mechanism, the method has often found use in estimating the rate constants for further kinetic analysis.

It is well known that XRD can be used to quantify crystalline phases in a mixture. The theoretical basis of quantitative XRD was developed by Klug and Alexander (13). It has been successfully used in several pharmaceutical systems (for example, ref. 16). In a mixture of two components, the intensity of line i of component 1, I_{i1}, is related to its weight fraction x_1, according to the equation:

$$\frac{I_{i1}}{(I_{i1})_0} = \frac{x_1\mu_1^*}{x_1(\mu_1^* - \mu_2^*) + \mu_2^*} \quad (1)$$

where $(I_{i1})_o$ is the intensity of line i in a sample consisting of only component 1, and μ_1^* and μ_2^* are the mass attenuation coefficients of components 1 and 2 respectively. If $\mu_1^* \cong \mu_2^*$ then equation (1) approximates to

$$\frac{I_{i1}}{(I_{i1})_0} = x_1 \quad (2)$$

Since, in the first reaction, ASH was transforming to ASA and in the second, ASA was decomposing to DKP, the quantitative analyses involved ASH - ASA and ASA - DKP mixtures. For the purposes of quantitative analyses, the mass attenuation coefficients of ASH (μ^*_{ASH}), ASA (μ^*_{ASA}) and DKP (μ^*_{DKP}) were calculated to be 6.61, 6.50 and 6.36 cm^2g^{-1} (Cu Kα radiation). These calculations were based on the molecular formulae of the 3 compounds (13). Since these values were quite close to one another, it was assumed that $\mu^*_{ASH} \cong \mu^*_{ASA} \cong \mu^*_{DKP}$.

Dehydration of ASH

While ASH has been subjected to detailed solid-state characterization studies (11,12), the kinetics of its dehydration to ASA has not been investigated. We studied the dehydration process isothermally, at several temperatures, over the range of 106 to 124°C. Fig. 2 shows the XRD patterns of ASH when it was maintained isothermally at 118°C.

Based on the large amount of sorbed water (~0.7% w/w) in the sample, it was suspected that the "as is" ASH was not completely crystalline (17). When the kinetic study was initiated by raising the sample temperature, there was an initial increase in the intensity of the peaks of ASH (see the data point at 1 min of ASH in Fig. 3). This could be attributed to the temperature induced recrystallization of ASH (i.e., annealing). While the recrystallization and dehydration processes are expected to occur simultaneously, the pronounced increase in peak intensity suggests that at the early stages of the reaction, the rate of crystallization >> the rate of dehydration. After the initial increase, the intensities of ASH peaks progressively decreased due to dehydration. This was accompanied by an increase in the intensity of the 17.1°2Θ peak of ASA.

To evaluate the dehydration kinetics of ASH, it was necessary to determine the fraction dehydrated (Eq. 2), as a function of time. This can only be accomplished if the intensities of the 15.9 and 16.4°2 Θ peaks of 100% crystalline ASH are known [$(I_{i1})_0$ in Eqn. 2; ASH being component 1]. Since the "as is" ASH was not completely crystalline, the $(I_{i1})_0$ value was obtained by extrapolation. When the sum of the intensities of the 15.9 and 16.4°2Θ peaks (on the log scale) were plotted as a function of time, the initial decrease in concentration (over the time range of 4 to 20 min) was approximately a first-order process (Fig. 4). Many solid-state reactions have been shown to follow first-order kinetics, for which Carstensen has provided the theoretical basis (18). These val-

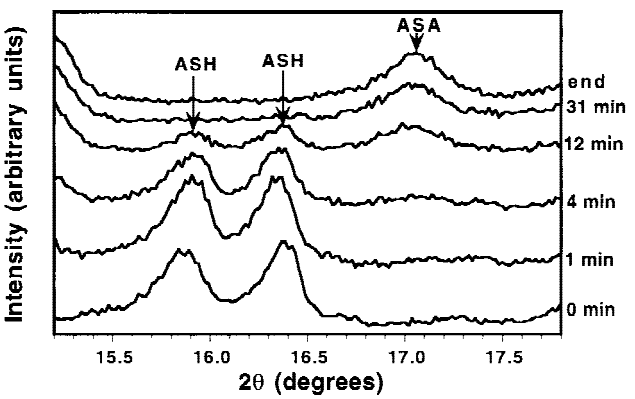

Fig. 2. Isothermal XRD of aspartame hemihydrate (ASH) at 118°C. The peaks unique to ASH and ASA are pointed. The XRD pattern marked 'end' was obtained after increasing the sample temperature to 150°C.

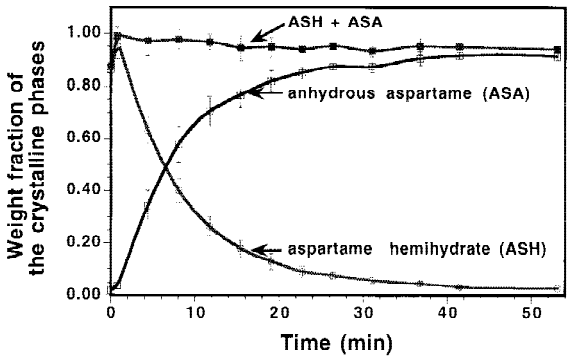

Fig. 3. Weight fractions of ASH and ASA as a function of time following storage of ASH at 118°C. Mean ± SD (n = 3). The curves are drawn only to assist in visualizing the trends.

ues were extrapolated (Fig. 4; inset) for the determination of $(I_{i1})_0$. Such an extrapolation assumes that when placed at high temperatures, ASH completely crystallizes within a few minutes. This assumption will be valid if the glass transition temperature (T_g) is substantially lower than the experimental temperature. Unfortunately, the T_g of ASH is not known. However, the assumption seems reasonable, in light of the high temperatures at which the experiments were conducted (106 to 124°C) and the high degree of crystallinity (> 85%; as calculated in the following paragraph) of the 'as is' ASH. We were able to compare the $(I_{i1})_0$ values obtained at different temperatures. Since the counting time (t_m) in the position sensitive detector was not constant, the extrapolated values of $(I_{i1})_0$ were normalized for the counting time. The $(I_{i1})_0/t_m$ values were pooled and determined to be 900 ± 26 counts/sec (mean ± SD; n = 10). The low standard deviation value suggests that the crystallinity of ASH is approximately constant in this temperature range and is likely to be close to 100%. In each experiment, the intensity of the ASH peaks at different time points were divided by $(I_{i1})_0$ (for that experiment) to obtain the weight fraction (x_1) of ASH (plotted in Fig. 3).

It was thus possible to determine the crystallinity of 'as is' ASH without the use of reference standards. Based on the initial x_1 value of 0.86 ± 0.03 (mean ± SD; n = 10), the crystallinity of ASH was ~86%.

The dehydration of ASH resulted in the formation of ASA and the intensity of the 17.1°2Θ peak enabled the quantification of ASA (Fig. 3). The peaks due to ASH had completely disappeared in less than 200 min and the intensity of 17.1°2Θ peak of ASA appeared to have reached a maximum value. However, the sample was maintained at the reaction temperature for a total of 500 min. No further changes were observed in the peak intensity. The sample temperature was increased to 150°C and held for 2 min. At this temperature, based on thermal analysis, rapid and complete dehydration is expected. Interestingly, the XRD pattern (Fig. 2; pattern marked 'end') revealed an increase in the intensity of the ASA peak. This increase could be due to either or both of the following reasons: (i) the dehydration reaction was not complete at 118°C and (ii) there was an increase in the crystallinity of ASA when the temperature was increased from 118°C to 150°C. Karl Fischer titrimetry of the sample, before heating it to 150°C, revealed negligible water content. Therefore, the increase in the peak intensity is attributed to an increase in the crystallinity of ASA. This sample was assumed to be 100% crystalline (justification provided later in the paragraph). The integrated intensity of the 17.1°2Θ peak at every time point was divided by the intensity of ASA peak at 150°C to obtain the weight fraction of the crystalline product (x_2) that was formed. These values are plotted as a function of time in Fig. 3. Since we were simultaneously quantifying the crystalline reactant as well as the reaction product, the sum of these two phases was also plotted (Fig. 3). The sum was less than unity at all time points. In order to determine the effect of temperature on the crystallinity of ASA, ASH was subjected to variable temperature XRD, over the temperature range of 130 to 170°C. The crystallinity, based on the integrated intensity of the 17.1°2Θ peak of ASA, increased up to 145°C and remained constant thereafter. This suggests that the crystallization is complete at 145°C. However, in the temperature range of the kinetic study (106 to 124°C), there was incomplete crystallization of ASA. Thus there is a significant amorphous content (up to 5% w/w at high temperatures and up to 10% w/w at low temperatures) in the sample throughout the dehydration process. Plots similar to Fig. 3 were obtained at several temperatures over the range of 106 to 124°C. The crystallinity of the product, ASA, increased as a function of temperature. Since XRD quantifies only the crystalline phases, the actual weight fractions of ASH and ASA (which include both the crystalline and amorphous components) cannot be accurately determined. It was therefore deemed inappropriate to fit the data to various solid-state reaction equations. However, the initial decrease in concentration of crystalline ASH as a function of time, approximated a first-order process (Fig. 4; inset).

For the determination of the dehydration rate constant, the mole fraction of crystalline ASH that has disappeared (i.e. dehydrated), α, was plotted (on the log scale) as a function of time. The use of Eq. 2 provided the weight fraction of ASH, which was transformed to α. Since, we were simultaneously quantifying the reactant and the reaction product (ASA), two independent determinations of α were performed and these were generally in excellent agreement. However, for the sake of simplicity, the α value based on the weight fraction of ASH was used to calculate the rate constant values. In the temperature range of the study (106–124°C) the dehydration of ASH appeared to be a first-order process. When the natural logarithm of first-order rate constants were plotted as a func-

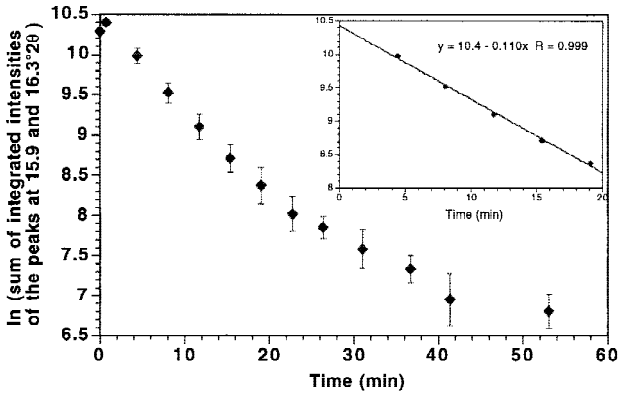

Fig. 4. Plot of the intensities of ASH peaks as a function of time at 118°C. The inset shows the same plot in the time range of 4 to 20 min. The y-intercept was used to obtain the value of $(I_{i1})_0$.

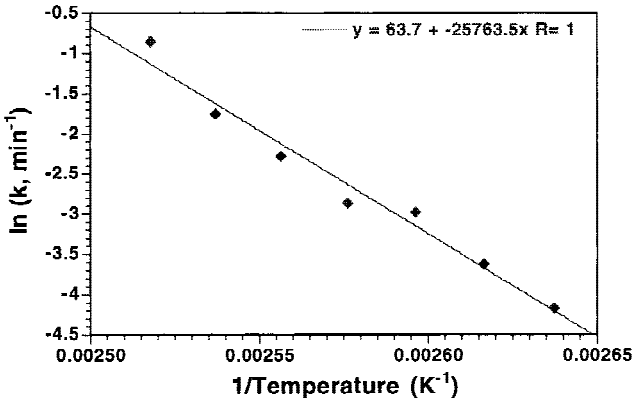

Fig. 5. Arrhenius plot for the dehydration of ASH.

tion of the inverse of the temperature, a linear relationship was observed (Fig. 5). The energy of activation for dehydration from the Arrhenius plot was calculated to be 214 kJ/mol. We emphasize that the fitting to the first-order equation was done not with the intent of determining the mechanism of dehydration but only to be able to obtain an approximate activation energy value.

Ng developed an approach for calculating the activation energy of a solid-state decomposition reaction without fitting the data to any kinetic equation (19). In this method, a plot of $\ln(t_{1/2})$ vs. 1/T must be linear and the value of Ea is calculated from the slope. Here $t_{1/2}$ is the time for 50% of the solid to decompose at temperature T. Using this approach, the value of Ea was determined to be 206 kJ/mol. This was in very good agreement with the value determined from the Arrhenius plot.

Decomposition of ASA Through Intramolecular Cyclization

Previously TGA was used to study the kinetics of the intramolecular cyclization of aspartame anhydrate (ASA) to form a diketopiperazine (DKP) derivative (9,10). The reaction was studied isothermally at several temperatures, in the temperature range of 160 to 185°C. The XRD patterns of ASA maintained isothermally at 160°C are presented and the peaks unique to ASA and DKP are pointed out (Fig. 6). The reaction was considered to be complete when the peaks due to ASA had completely disappeared and that due to DKP had attained the maximum possible intensity. To confirm the completion of the reaction, the final product was heated to 195°C, held for 5 min, and the XRD pattern was obtained (Fig. 6; pattern labeled as 'End'). At this temperature, based on thermal analysis, rapid and complete degradation is expected. The integrated intensities of the 13.0°2Θ peaks of DKP before and after increasing the temperature to 195°C were compared. In all cases, the two intensity values were identical indicating that (i) at all the experimental temperatures (160 to 185°C), the reaction had gone to completion, and (ii) the crystallinity of the DKP formed was the same in the temperature range of 160 to 195°C. The latter observation strongly suggests that DKP formed was completely crystalline (~100% crystallinity). The high crystallinity of DKP is also evident from its XRD pattern (Fig. 1) which consists of sharp peaks and by the absence of regions of amorphous halo.

Using Eq. 2, it is possible to calculate the weight fractions of ASA and DKP. The integrated intensity of the unique

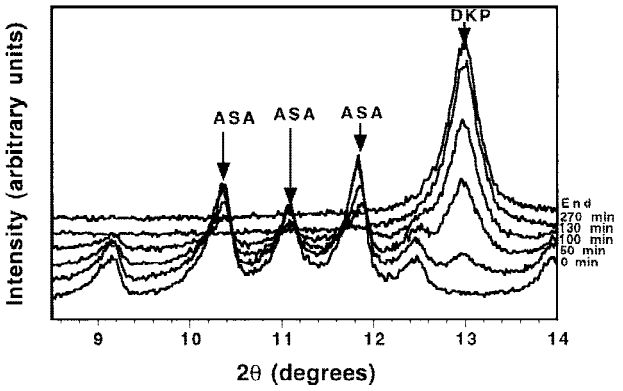

Fig. 6. Isothermal XRD of ASA at 160°C. The anhydrate undergoes intramolecular cyclization to form DKP. Some unique peaks of the anhydrate and one unique peak of DKP are pointed out.

XRD peaks of the initial ASA sample gave the value of $(I_{i(ASA)})_0$. Similarly the value of $(I_{i(DKP)})_0$ was obtained from the value of integrated intensity of its unique XRD peak at the end of the reaction (pattern labeled as 'End' in Fig. 6). As mentioned earlier, at any time during the course of the reaction, dividing the integrated intensity of the peak unique to any phase by that of the pure phase, yielded its weight fraction (Eq. 2). Since the weight fractions of the crystalline reactant and product had been simultaneously determined, the sum of the two was plotted as a function of time (Fig. 7). At all time points, this was close to unity ($< \pm 0.02$). This reveals that the concentration of amorphous intermediate(s), if any, is very low. While Fig. 7 is one representative example, similar plots were generated at all other temperatures of study. The kinetic data in the range of $0.1 \leq \alpha \leq 0.9$ were fitted to the various solid-state reaction models. The data in the range of $\alpha < 0.1$ and $\alpha > 0.9$ were deemed unsuitable for the modeling studies (20). The best fit was obtained with the nucleation controlled models described by Avrami-Erofe'ev (3-dimensional growth) and Prout-Tompkins. This conclusion was based on the value of the coefficient of correlation, r, obtained after the data fitting. These findings are in agreement with the earlier observations of Leung and Grant (9). A unique advantage of XRD is that the value of α (mole fraction of reactant that has disappeared) was obtained both by measuring the concentration of ASA and also from the concentration of DKP (reaction product). The rate constant values obtained from these 2 independent determinations were

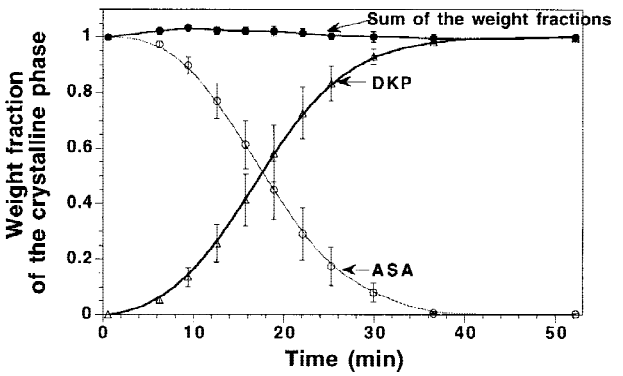

Fig. 7. Weight fractions of ASA and DKP as a function of time, following storage of ASA at 180°C. Mean ± SD (n = 3).

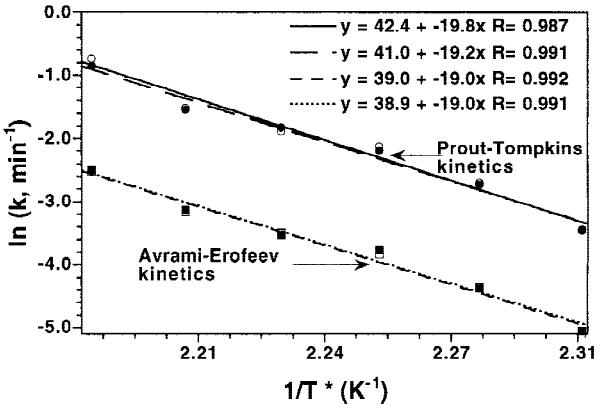

Fig. 8. Arrhenius plots for the intramolecular cyclization of ASA for nucleation controlled models described by Prout-Tompkins (circles) and Avrami-Erofeev (squares) equations. The closed and open legends represent the data obtained from the concentration of the reactant (ASA) and the product (DKP) respectively.

very close to each other. These rate constants were used to draw the Arrhenius plots (Fig. 8). The activation energy (Ea) was calculated to be 160 kJ/mol. This was significantly different from the Ea value of 268 kJ/mol obtained from TGA (9). This difference may be attributed to one or more of the following reasons.

The amount of sample used in XRD is almost an order of magnitude higher than that in TGA. An inverse relationship between sample weight and activation energy of endothermic reactions has been observed which was attributed to the greater self-cooling effect of larger sample mass (21,22). As mentioned earlier, a characteristic feature of solid-state thermal decomposition reactions is that the course of the reaction is affected by preparation and handling of the sample as well as by the surrounding gas atmosphere. The sample packing for the TGA was different from that for the XRD. In the TGA, the sample was packed loosely, while in the XRD holder, the sample was tightly packed into the holder so as to maximize the diffracted peak intensity. The raw materials (ASH) used in the studies were from two different lots. Differences in particle size, geometry and surface characteristics can alter the reaction rates. Finally, during the TGA, the sample was purged with nitrogen. The XRD experiments were carried out under static conditions.

A unique advantage of this technique is that the two reaction steps were completely carried out *in situ* in the sample chamber of the XRD. This enabled us to avoid the variability and errors due to sample packing. Moreover, there was no need for an internal standard. The addition of an internal standard can cause several difficulties. Homogenous mixing of solid powders is difficult to achieve. In addition to increasing the time for sample preparation, mechanical mixing of the sample with an internal standard can induce lattice disorder in the analyte, and in extreme cases, cause its phase transformation. The presence of an internal standard might alter the reaction kinetics, and at elevated temperatures, there was the risk of chemical interactions between the internal standard and the analytes. In order to avoid these problems, at each time point, the sample must be cooled to room temperature, and subjected to XRD after the addition of the internal standard. This would necessitate the preparation of a fresh sample at each time point, which would have obviated all the advantages of the technique.

CONCLUSIONS

Variable temperature XRD is a powerful tool to probe reactions in solid pharmaceuticals. The technique not only reveals the formation of intermediates during the reactions but also provides information about their solid-state. XRD was successfully used to simultaneously quantify the, (i) disappearance of aspartame hemihydrate (ASH) and appearance of aspartame anhydrate (ASA) in the first reaction, and (ii) disappearance of ASA and appearance of a diketopiperazine derivative (DKP) in the second reaction. In the first situation (dehydration of ASH), XRD revealed that the reactant (i.e., ASH) was incompletely crystalline and yielded a product (ASA) which was not fully crystalline. Interestingly, the crystallinity of the reaction product increased as a function of the dehydration temperature until it attained the maximum value at ~145°C. Because of the crystallinity issue, this XRD based quantification technique was not deemed to be the most appropriate method for evaluating the reaction kinetics. Still, the technique provided insight into the reaction mechanism and the solid-state of the reacting species - information unlikely to be obtained from conventional thermoanalytical techniques. XRD was an ideal technique to study the kinetics of cyclization of ASA to form DKP. This was a nucleation controlled process with an activation energy of 160 kJ/mol. The excellent mass balance at all the time points of the reaction indicates the absence of intermediate phases. The wealth of information provided by XRD makes it an invaluable tool in the investigation of solid-state reactions. However, despite the advantages, one must be aware that XRD directly quantifies only the crystalline components.

ACKNOWLEDGMENTS

The helpful comments of Dr. David Grant (University of Minnesota) and Dr. Raymond Skwierczynski (3M Pharmaceuticals, St. Paul, MN) are gratefully acknowledged.

REFERENCES

1. J. L. Ford and P. Timmins. *Pharmaceutical Thermal Analysis: Techniques and Applications,* Ellis Harwood Limited, Chichester, UK, 1993.
2. D. Giron. Themal analysis and calorimetric methods in the characterization of polymorphs and solvates. *Thermochim. Acta*. **348**: 1–59 (1995).
3. J. Han and R. Suryanarayanan. Influence of environmental conditions on the kinetics and mechanism of dehydration of carbamazepine dihydrate. *Pharm. Dev. Tech*. **3**:587–596 (1998).
4. S. Rastogi, M. Zakrzewski, and R. Suryanarayanan. Use of high temperature X-ray powder diffractometry (XRD) to investigate complex solid-state reactions. *Pharm. Res*. **14**:S192 (1997).
5. J. Nishijo and F. Takenaka. Studies of the properties of the complex medicines. I. Differential thermogravimetric analysis of aminophylline. *J. Pharm. Soc. Jap*. **99**:824–829 (1979).
6. J. Nishijo, H. Minamiguchi, and R. Moriya. Solid complex of theophylline with trimethylenediamine. *J. Pharm. Soc. Jap*. **100**: 157–161 (1979).
7. N. V. Phadnis and R. Suryanarayanan. Polymorphism in anhydrous theophylline—Implications on the dissolution rate of theophylline tablets. *J. Pharm. Sci*. **86**:1256–1263 (1997).
8. H. Hashizume, S. Shimomura, H. Yamada, T. Fujita, and H. Nakazawa. An X-ray diffraction system with controlled relative humidity and temperature. *Powder Diffr.* **11**:288–289 (1996).

9. S. S. Leung and D. J. W. Grant. Solid state stability studies of model dipeptides: aspartame and aspartylphenylalanine. *J. Pharm. Sci.* **86**:64–71 (1997).
10. R. D. Skwierczynski., Disorder, molecular mobility, and solid-state kinetics: the two-environment model. *J. Pharm. Sci.* **88**: 1234–1236 (1999).
11. S. S. Leung, B. E. Padden, E. J. Munson, and D. J. W. Grant. Solid state characterization of two polymorphs of aspartame hemihydrate. *J. Pharm. Sci*. **87**:501–507 (1998).
12. S. S. Leung, B. E. Padden, E. J. Munson, and D. J. W. Grant. Hydration and dehydration behavior of aspartame hemihydrate. *J. Pharm. Sci*. **87**:508–513 (1998).
13. P. L. Klug and L. E. Alexander. *X-ray Diffraction Procedures for Polycrystalline and Amorphous Materials,* Wiley, New York, 1974.
14. S. K. Rastogi, *Phase Transitions and Decomposition Reactions in Pharmaceutical Solids.* Ph.D. Dissertation, University of Minnesota, Minneapolis, MN, 2000.
15. J. H. Sharp, G. W. Brindley, and B. N. N. Achar. Numerical data for some commonly used solid state reactions. *J. Am. Ceram. Soc*. **52**:781–791 (1963).
16. R. Suryanarayanan, Determination of the relative amounts of anhydrous carbamazepine ($C_{15}H_{12}N_2O$) and carbamazepine dihydrate ($C_{15}H_{12}N_2O \cdot H_2O$) in a mixture by powder X-ray diffractometry. *Pharm. Res*. **6**:1017–1024 (1989).
17. C. Ahlneck and G. Zografi. Molecular basis of moisture effects on the physical and chemical stability of drugs in the solid state. *Int. J. Pharm*. **62**:87–95 (1990).
18. J. T. Carstensen. Stability of solids and solid dosage forms, *J. Pharm. Sci*. **63**:1–14 (1974).
19. W. Ng. Thermal decomposition in the solid state. *Aust. J. Chem*. **28**:1169–1178 (1975).
20. P. Jacobs and F. Tompkins. Classification and theory of solid reactions. In G. Garner (ed.), *Chemistry of the Solid-State,* Academic Press, New York, 1955 pp. 184–212.
21. P. K. Gallagher and D. W. Johnson, Jr. The effects of sample size and heating rate on the kinetics of the thermal decomposition of $CaCO_3$. *Thermochim. Acta* **6**:67–83 (1973).
22. C. O. Agbada and P. York. Dehydration of theophylline monohydrate powder—Effects of particle size and sample weight. *Int. J. Pharm*. **106**:33–40 (1994).